Imaging-based evaluation of liver function: comparison of ^{99m}Tc-mebrofenin hepatobiliary scintigraphy and Gd-EOB-DTPA-enhanced MRI

Dominik Geisel · Lutz Lüdemann · Vera Fröling · Maciej Malinowski ·
Martin Stockmann · Annekathrin Baron · Bernhard Gebauer ·
Daniel Seehofer · Vikas Prasad · Timm Denecke

Abstract

Objectives To compare Gd-EOB-enhanced MRI and ^{99m}Tc-mebrofenin hepatobiliary scintigraphy (HBS) as imaging-based liver function tests for separate evaluation of right (RLL) and left liver lobe (LLL) function.

Methods Fourteen patients underwent Gd-EOB-enhanced MRI and ^{99m}Tc-mebrofenin HBS after portal vein embolization within 24 h. Relative enhancement (RE) and hepatic uptake index (HUI) were determined from MRI; and T_{max}, $T_{1/2}$ and mebrofenin uptake were determined from HBS, all values separately for RLL and LLL.

Results Mebrofenin uptake correlated significantly with HUI and RE for both liver lobes. There was strong correlation of mebrofenin uptake with HUI for RLL ($r^2=0.802$, $p=0.001$) and RE for LLL ($r^2=0.704$, $p=0.005$) and moderate correlation with HUI for LLL ($r^2=0.560$, $p=0.037$) and RE for RLL ($r^2=0.620$, $p=0.018$). Correlating the percentage share of RLL function derived from MRI (with HUI) with the percentage of RLL function derived from mebrofenin uptake revealed a strong correlation ($r^2=0.775$, $p=0.002$).

Conclusions Both RE and HUI correlate with mebrofenin uptake in HBS. The results suggest that Gd-EOB-enhanced MRI and ^{99m}Tc-mebrofenin HBS may equally be used to separately determine right and left liver lobe function.

Key points
• *Information about liver function can be acquired with routine Gd-EOB-MRI.*
• *Gd-EOB-MRI and ^{99m}Tc-mebrofenin HBS show elevated function of non-embolized lobe.*
• *Gd-EOB-MRI and ^{99m}Tc-mebrofenin HBS can determine lobar liver function.*

Keywords MRI · Liver function · Mebrofenin scintigraphy · EOB · Gadoxetic acid

D. Geisel (✉) · V. Fröling · B. Gebauer · T. Denecke
Department of Diagnostic and Interventional Radiology, Charité
Campus Virchow-Klinikum, Augustenburger Platz 1,
13353 Berlin, Germany
e-mail: dominik.geisel@charite.de

V. Fröling · V. Prasad · T. Denecke
Department of Nuclear Medicine, Charité Campus
Virchow-Klinikum, Augustenburger Platz 1, 13353 Berlin, Germany

L. Lüdemann
Department of Medical Physics, Essen University Hospital,
Hufelandstraße 55, 45147 Essen, Germany

M. Malinowski · M. Stockmann · A. Baron · D. Seehofer
Department of General, Visceral and Thoracic Surgery, Charité
Campus Virchow-Klinikum, Augustenburger Platz 1,
13353 Berlin, Germany

Abbreviations

FRL	future remnant liver
Gd-EOB-	gadolinium ethoxybenzyl
DTPA	diethylenetriaminepentaacetic acid
HBS	hepatobiliary scintigraphy
HUI	hepatic uptake index
ICG	indocyanine green
LLL	left liver lobe
PVE	portal vein embolization
RE	relative enhancement
RLL	right liver lobe
ROI	region of interest
SI	signal intensity
VIBE	volume interpolated breath-hold examination

Introduction

An imaging-based liver function test capable of determining liver function on a regional level and allowing prediction of both postoperative liver function and the risk of postoperative liver failure would be a powerful tool for hepatologists and liver surgeons [1–8]. Liver resections for hepatic malignancies become more radical to achieve a curative therapy for an increasing number of patients [9]. These more radical therapies lead to a higher risk of postoperative liver failure. If volumetry and global liver function tests like indocyanine green (ICG) or LiMAx show a high risk of postoperative liver failure, portal vein embolization (PVE) is an established method to increase future remnant liver (FRL) volume and decrease the incidence of postoperative liver failure, allowing more patients with an otherwise small FRL volume to benefit from partial resection [9–14]. After PVE, however, liver function is no longer distributed equally over the liver tissue [5]. Additionally, liver function may be compromised by e.g. preoperative chemotherapy or chronic cholestasis. An imaging-based liver function would be the ideal tool to estimate the FRL function, to monitor the success of PVE, to schedule the time of surgery, and to identify patients at an increased risk for postoperative liver failure.

Scintigraphic methods—mostly using ^{99m}Tc-IDA (iminodiacetate) analogues like mebrofenin as tracers—are currently the only imaging-based liver function tests used to assess liver uptake and biliary excretion of tracers in clinical practice [15–17]. Dynamic ^{99m}Tc-mebrofenin hepatobiliary scintigraphy (HBS) or single photon emission computed tomography (SPECT) can be used to estimate total liver function and to predict postoperative remnant liver function of residual liver volume [6, 18]. Furthermore, HBS can be used to monitor the increase in function of the remnant liver following preoperative PVE and correlates with the ICG clearance test [2, 5, 6, 18, 19]. Problems with scintigraphic methods are low temporal and spatial resolution and the overlap of left and right sectors because of planar acquisition [17].

Gd-EOB-DTPA (gadolinium ethoxybenzyl diethylenetriaminepentaacetic acid) is a magnetic resonance imaging (MRI) contrast agent that shares several pharmacokinetic properties with IDA—both are taken up by hepatocytes through the organic anionic transport system (OATS) and are excreted into the bile by glutathione S-transferase. Therefore, Gd-EOB-enhanced MRI is being developed as an alternative to the established scintigraphic methods but is not yet available for routine clinical use [3, 4, 20, 21]. Potential advantages include that there is no need for a radioactive tracer and that the examination can be integrated into routine preoperative workflow. Moreover, state-of-the-art MRI sequences provide superior temporal and spatial resolution compared to SPECT-CT. By increasing the flip angle, the signal ratio of Gd-EOB to background can be increased substantially to enable an acquisition quite similar to HBS [22]. However, as Gd-EOB-DTPA is also eliminated by renal excretion (approx. 50 %), there is the need for an investigation to quantitatively compare the hepatic uptake measured by HBS and EOB-MRI in normal and functionally impaired liver tissue to ensure equal ability of EOB-MRI with regards to liver function testing before starting further efforts to develop a sophisticated EOB-MRI liver function quantification tool [23]. This requires prospective testing with both modalities in subjects with different liver function in the left and right lobe to allow for an intraindividual analysis of uptake differences reliably quantifiable by HBS as the reference method and by EOB-MRI.

Therefore the purpose of this study was to compare static Gd-EOB-DTPA-enhanced MRI with ^{99m}Tc-mebrofenin HBS as imaging-based liver function tests. PVE served as a model for heterogeneous distribution of liver function where the separate right and left liver lobe function was evaluated.

Materials and methods

Patients treated with right PVE between July 2010 and March 2014 and underwent ^{99m}Tc-mebrofenin HBS and Gd-EOB-enhanced MRI within 24 h were retrospectively enrolled in our study. The study complied with the Declaration of Helsinki. The study protocol was approved by the institutional review board.

^{99m}Tc-mebrofenin HBS

All examinations were performed on a SPECT/CT system (Symbia T6, Siemens Healthcare, Erlangen, Germany). An unenhanced low-dose CT of the upper abdomen was obtained for planning. The CT images were evaluated to determine the individual scan fielding z-axis and the right anterior oblique rotation angle of the detector according to the line separating the left and right liver lobe (reference structures: middle hepatic vein, gall bladder, inferior vena cava). After intravenous administration of 185 MBq ^{99m}Tc-mebrofenin (Bridatec, GE Healthcare), dynamic image acquisition was performed with the liver and heart in the field of view (FOV) using a single low energy high resolution collimator (energy window, 130–150 keV; matrix, 64×64). Dynamic acquisition was performed over 45 min at 30 s per frame (90 frames).

Regions of interest (ROIs) were drawn around right liver lobe and left liver lobe and heart/large vessels within the mediastinum as blood pool. Liver ROIs were drawn manually by one experienced radiologist and nuclear medicine physician with 10 years of experience. The parameters T_{max} and $T_{1/2}$ were obtained from the time–activity curve of the right and left liver lobe. Liver uptake of mebrofenin was calculated as the increase in blood-pool-corrected ^{99m}Tc-mebrofenin

uptake per minute from 150 to 350 s after injection (total duration of 200 s) to ensure that the calculations are made during a phase of homogeneous distribution of the agent in the blood pool, before biliary excretion takes place, as described by Bennink et al. [6, 18, 24]. The percentage function of the right and left liver lobe was calculated by multiplying mebrofenin liver uptake U of the right or left liver lobe by the appropriate lobar volume V from prior AC-CT, similar to the hepatic uptake index (HUI) in MRI, and then setting these values in proportion with the following formula (exemplarily for RLL):

$$U_{RLL} \times V_{RLL}/[U_{RLL} \times V_{RLL} + U_{LLL} \times V_{LLL}].$$

MRI

Gd-EOB-DTPA-enhanced MRI was performed within 24 h before or after HBS. MRI was acquired on a 1.5-T-device (Avanto, Siemens, Erlangen, Germany) using and an eight-channel body phased-array coil. A standard volume interpolated breath-hold examination sequence (VIBE) in the axial plane with a TR of 4.26 ms, a TE of 1.87 ms, a flip angle (FA) of 10°, a slice thickness 3 mm and a matrix size of 256×127 was acquired covering the entire liver with 60–72 slices and an adjusted field of view (FOV) of 255–300×340–400 mm. A dose of 0.1 mL Gd-EOB-DTPA (0.25 mmol/mL) per kg body weight was then manually injected in an anterior cubital vein, followed by a saline flush of 20 mL. After 20 min in the hepatocyte phase, the standard VIBE sequence was repeated.

Images were evaluated with OsiriX version 5.8 (Pixmeo SARL, Bernex, Switzerland). MRI was evaluated by one experienced radiologist and nuclear medicine physician with 10 years of experience. Five representative circular regions of interest (ROIs) with a fixed diameter of 3 cm were placed on the images in both the left (territory of the left nonembolized portal vein) and the right liver lobe (territory of the embolized right portal vein) and the spleen, avoiding large vessels and liver lesions such as cysts or tumours. ROIs were placed in different parts of the liver lobe to minimize gravity and magnetic heterogeneity effects. Relative enhancement was calculated by subtracting the signal intensity (SI) of the unenhanced images from the SI in the hepatobiliary phase and dividing the difference by the SI of the unenhanced images [25]. Volume (V) was measured manually delineating both the RLL and the LLL, virtually separated by the planned resection line. Tumour masses, large vessels or bile ducts and other liver lesions were excluded from the volume. As introduced by Yamada et al. [7], the HUI for RLL and LLL was calculated according to the following formula: $V_{Liver} [(SI_{Liver}/SI_{Spleen})-1]$, where V_L and SI_L were taken either for RLL or for LLL. The percentage function of the right and left liver lobe was calculated according to the proportions of HUI for RLL and LLL.

Statistical analysis

Statistical analysis was performed using PASW Statistics 22 (IBM, Armonk, New York). The t test and Wilcoxon signed-rank test for paired values were applied to compare features of RLL and LLL. Correlations were tested by calculating Spearman Rho correlation coefficients. A two-sided test was used for assessing statistical significance assuming significance at a p value of less than 0.05. Unless otherwise indicated, all quantitative data are expressed as mean±standard deviation.

Results

Patient characteristics

During the interval from July 2010 and March 2014, 14 patients (five women, nine men) were included in our study. Mean patient age was 59.2±10.3 years (range 45–83). The indication for HBS and MRI was planned extended liver resection after PVE in all cases. Reasons for resection were colorectal liver metastases in four patients and cholangiocarcinoma in ten patients. Average time from PVE to HBS and MRI was 15.2±2.1 days. Total serum bilirubin at the time of PVE was 1.4±1.23 mg/dL (range, 0.4–3.9; normal, <1.2 mg/dL) and was elevated in two patients because of cholestasis. No patient had clinical or morphologic signs of cirrhosis or other diffuse liver diseases. Serum creatinine at the time of PVE was 0.77±0.18 mg/dL (range, 0.52–1.1; normal, <1.2 mg/dL).

Results of ^{99m}Tc-mebrofenin HBS

Average T_{max} was 979.3±537.8 s for RLL and 848.6±295.7 s for LLL (Table 1). Average $T_{1/2}$ was 2,244.3±695.4 s for RLL and 2,011.6±626 s for LLL. Mebrofenin uptake in %/min was 10.54±4.26 %/min for RLL and 13.76±3.65 %/min for LLL. The difference between RLL and LLL for T_{max} and $T_{1/2}$ was not statistically significant (p=0.209 and 0.070, respectively). However, mebrofenin uptake was significantly higher for LLL than for RLL (p=0.001). The average share of total function was 49.02±12.68 % for RLL and 50.98±12.68 % for LLL.

Results of Gd-EOB-enhanced MRI

The average size of the RLL was 989.7±203.6 cm^3 and the average size of the LLL was 753.9±230.9 cm^3. Average unenhanced SI for RLL was 285.4±61.9 and 266.0±78.5 for LLL. Average SI in the hepatobiliary phase was 441.1±138.3 for RLL, 446.2±133.7 for LLL and 271±120.1 for the spleen. Average RE was 0.49±0.17 for RLL and 0.66±0.22 for LLL. Average HUI was 778.7±674.4 for RLL and 547.6±

Table 1 Parameters derived from ^{99m}Tc-mebrofenin hepatobiliary scintigraphy and Gd-EOB-enhanced MRI as well as volumes for right liver lobe (RLL) and left liver lobe (LLL)

T_{max} (s)		$T_{1/2}$ (s)		Mebrofenin uptake (%/min)		Relative enhancement		Hepatic uptake index		Volume (cm^3)	
RLL	LLL	RLL	LLL	RLL	LLL	RLL	LLL	RLL	LLL	RLL	LLL
979.3±537.8	848.6±295.7	2,244.3±695.4	2,011.6±626	10.54±4.26	13.76±3.65	0.49±0.17	0.66±0.22	778.7±674.4	547.6±352.1	989.7±203.6	753.9±230.9

352.1 for LLL. RE for LLL was significantly higher than for RLL ($p>0.001$). HUI did not differ statistically significantly between RLL and LLL ($p=0.066$). The average share of total function as indicated by HUI was 57.43±21.23 % for RLL and 42.57±21.23 % for LLL.

Correlation of scintigraphy and MRI

Both T_{max} and $T_{1/2}$ showed negative correlations with RE and HUI, but none of these were statistically significant. Mebrofenin uptake showed statistically significant correlations with HUI and RE for both liver lobes (Figs. 1 and 2). Strong correlation with HUI was calculated for RLL ($r^2=0.802$, $p=0.001$) and with RE for LLL ($r^2=0.704$, $p=0.005$); furthermore, moderate correlation with HUI for LLL ($r^2=0.560$, $p=0.037$) and RE for RLL ($r^2=0.620$, $p=0.018$) was revealed. Correlating the percentage share of RLL function derived from MRI (from the proportion of HUI) with the percentage share of RLL function derived from mebrofenin uptake revealed a strong correlation ($r^2=0.775$), which was statistically significant ($p=0.002$) (Fig. 3).

Discussion

We compared static Gd-EOB-DTPA-enhanced MRI with ^{99m}Tc-mebrofenin HBS as imaging-based liver function tests for the separate evaluation of right and left liver lobe function following PVE as a model for heterogeneous distribution of liver function in 14 patients.

T_{max} and $T_{1/2}$ derived from scintigraphy correlated negatively with HUI and RE, but this correlation was not statistically significant. This can be explained by the fact that they are too dependent on blood flow parameters and biliary congestion. Since mebrofenin and Gd-EOB are both taken up into hepatocytes through the OATS, which plays a key role in liver function, mebrofenin uptake and RE from Gd-EOB-enhanced MRI show strong correlation. The HUI is a measure of relative enhancement corrected for blood flow and liver volume, which explains the similar strength of correlation with mebrofenin uptake. Multiplying lobar mebrofenin uptake with lobar volume—similar to HUI—enables separate determination of left and right liver function from scintigraphy.

Imaging-based liver function tests represent a major improvement on global liver function tests such as the LiMAx or ICG test. The latter tests are unreliable in patients with regional dysfunction or heterogeneous distribution of liver function and are therefore unable to correctly predict postoperative liver function after PVE. Using ^{99m}Tc-mebrofenin SPECT combined with dynamic planar acquisition, de Graaf et al. showed that the increase in FRL function after PVE is higher than the increase in FRL volume, underlining the need for an
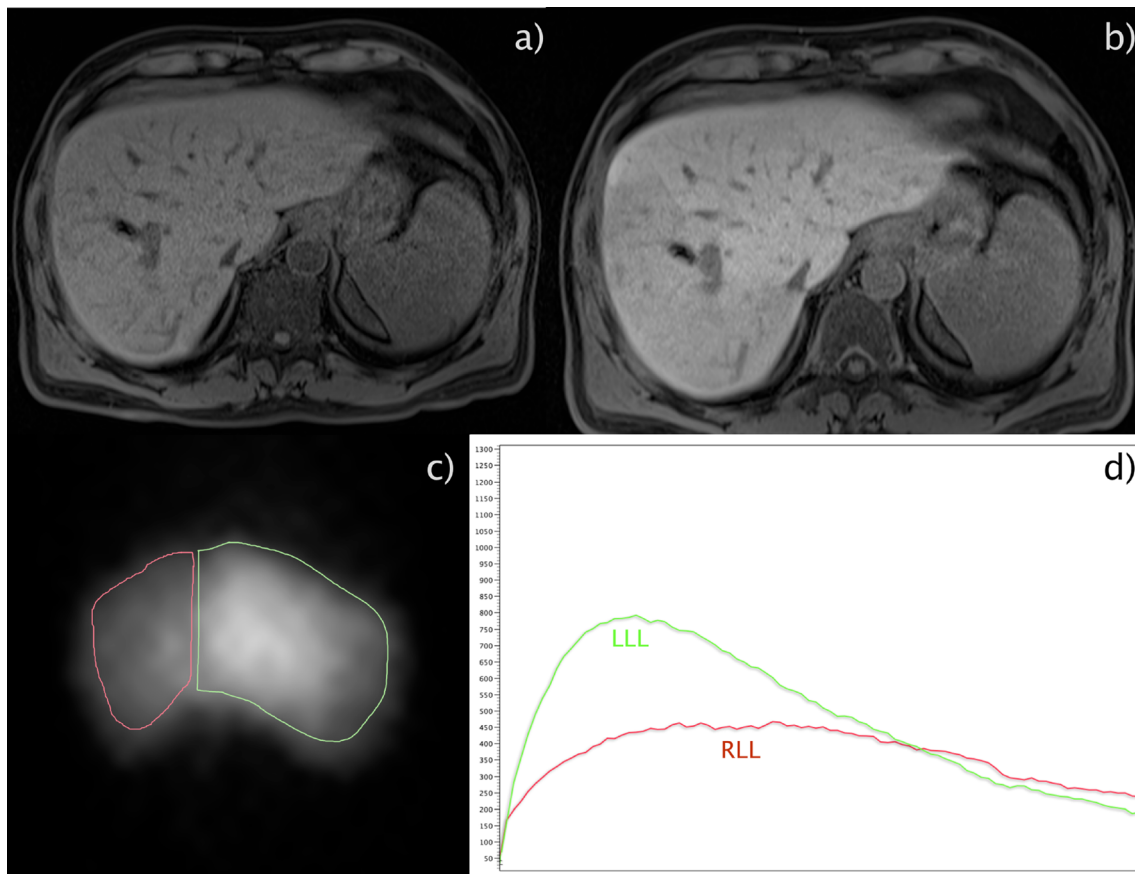
Fig. 1 67-year-old patient with colorectal liver metastasis scheduled for extended right liver resection; portal vein embolization was performed 2 weeks before. **a** Unenhanced and **b** Gd-EOB-enhanced MRI (T1 VIBE). **c** ^{99m}Tc-mebrofenin hepatobiliary scintigraphy after 10 min. **d** Liver uptake time–activity curve for RLL (*red*) and LLL (*green*)

image-based liver function test [5]. In recent years, increasing evidence has emerged to suggest that Gd-EOB-enhanced MRI can be used to determine liver function [3, 7, 21, 26–34]. However, there still exists no consensus on which parameter derived from MRI is the most suitable. The parameters that have been proposed include relative enhancement, HUI, absolute uptake determined by T1-mapping, hepatic extraction fraction and input relative blood flow [4, 7, 33, 34]. Relative enhancement and hepatic uptake index are two parameters that can be derived from virtually any Gd-EOB-enhanced MRI. Both have been shown to correlate with results of the ICG test and distinguish between normal and elevated MELD scores, which is why we chose these two parameters for our study [33–35].

When ^{99m}Tc-mebrofenin HBS is performed, the two most commonly used parameters to determine liver function are mebrofenin clearance (MCR) and uptake (MUR) rate. Both provide similar results relative to clearance rate expressed as millilitres per minute. The MUR is used in all clinical application to date [24]. Functional estimation with ^{99m}Tc-mebrofenin HBS is sufficient to predict postoperative outcome more accurately than by using liver volumetry [2]. By combining dynamic planar imaging and static three-dimensional imaging with SPECT, de Graaf et al. were able to visualize the functional increase per millilitre liver volume in the remnant liver following preoperative PVE [5]. This functional gain was also shown with Gd-EOB-enhanced MRI [8]. We did not use SPECT acquisition because our primary goal was the separation of right and left liver function, which can be achieved by rotating the detector to a right anterior oblique position determined by prior CT [36].

Gd-EOB-enhanced MRI has several advantages over ^{99m}Tc-labelled mebrofenin scintigraphy. First, it does not rely on a radioactive tracer, which makes it easier to conduct and avoids radiation exposure for the patient. Second, it easily integrates into preoperative clinical workflow. Gd-EOB-enhanced MRI is already conducted in an increasing number of patients scheduled for liver surgery since it not only provides morphological information but also allows highly sensitive tumour detection and assessment of topography with the intrahepatic vessels [37, 38]. Gd-EOB-enhanced MRI yields all the information required for preoperative planning with the functional information that can be derived from the data sets providing an additional bonus. Third, MRI has a superior
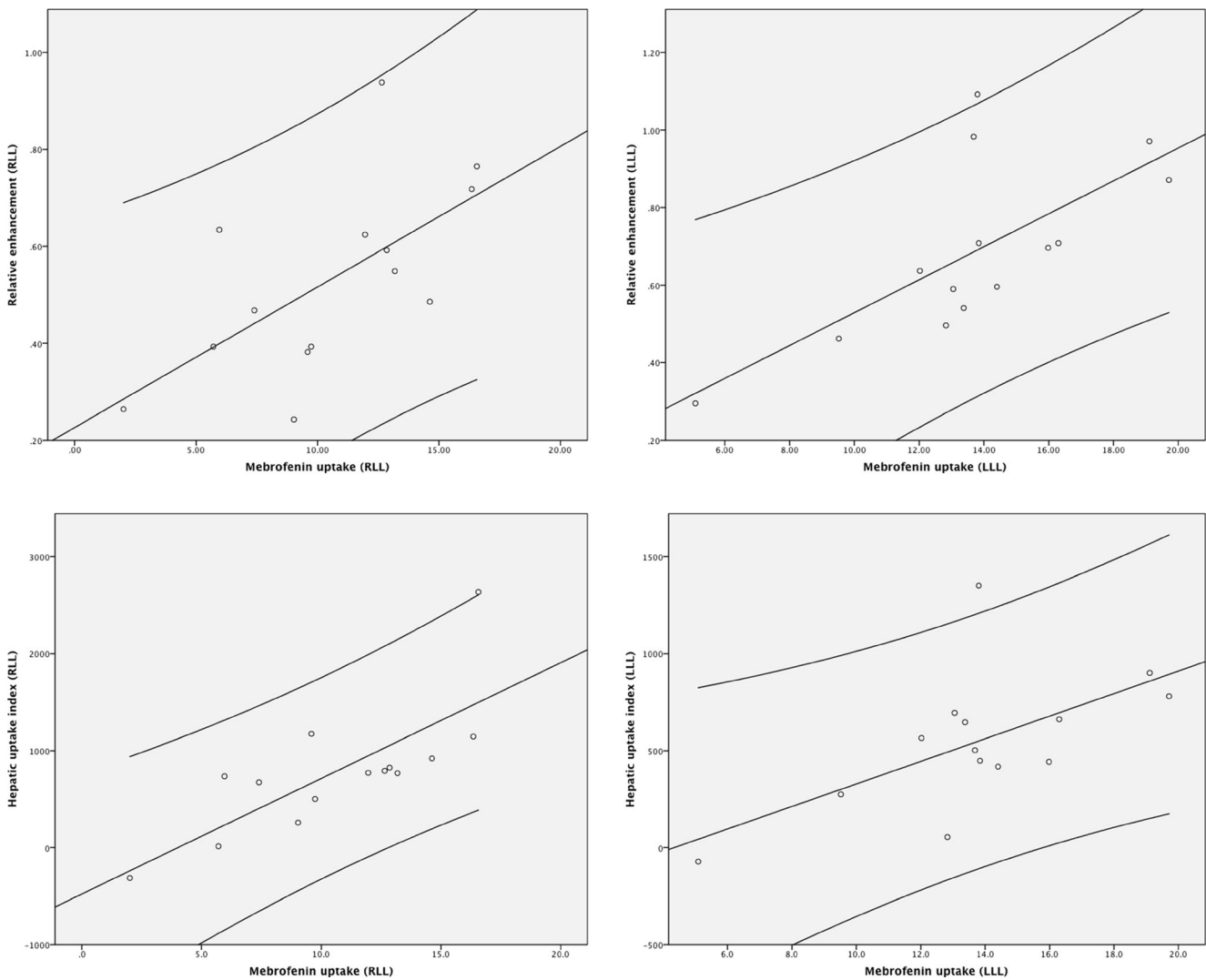
Fig. 2 Scatter plots show the correlation of relative enhancement or hepatic uptake index with mebrofenin uptake (%/min) for right and left liver lobe. Lines of best fit and 95 % confidence intervals are shown as *straight* and *curved lines*, respectively

temporal and spatial resolution. When novel sequences such as CAIPIRINHA-Dixon-TWIST are used, up to 14 high spatial resolution three-dimensional data sets (1.2×1.2×3 mm× 21 slices) can be acquired within 29 s [39]. This will enable precise calculation of hepatic extraction fraction from Gd-EOB-enhanced MRI in the near future.

Our study has several limitations. First, the study design was retrospective and the patient number was small, which can be explained by the still small number of patients undergoing ^{99m}Tc-mebrofenin HBS. Second, we were not able to correlate Gd-EOB uptake with mebrofenin uptake as MRI was only conducted at two time points (unenhanced and 20 min after contrast injection). A dynamic MRI study with high temporal resolution is needed to calculate Gd-EOB uptake and extraction fraction. Another weakness is that the reliability of both methods may be reduced in patients with elevated bilirubin; two patients had elevated bilirubin because

of obstruction. It is assumed that Gd-EOB-DTPA and mebrofenin compete with bilirubin for uptake, similar to ICG. Last, correlation with postoperative liver function as a "gold standard" would be highly desirable. This is, however, difficult to achieve as a perfect liver function test does not exist.

Although the correlation of HUI and mebrofenin uptake was significant, the average functional share of right and left liver lobe differed as average RLL function determined by MRI was 49.02±12.68 % versus 57.43± 21.23 % by HBS. A possible explanation could be the so-called attenuation bias resulting from the fact that the right liver lobe generally has a larger diameter than the left liver lobe, even when the gamma camera is rotated into right-anterior oblique orientation based on the individual patient's line separating the left and right liver lobe. This drawback can be overcome by simultaneous
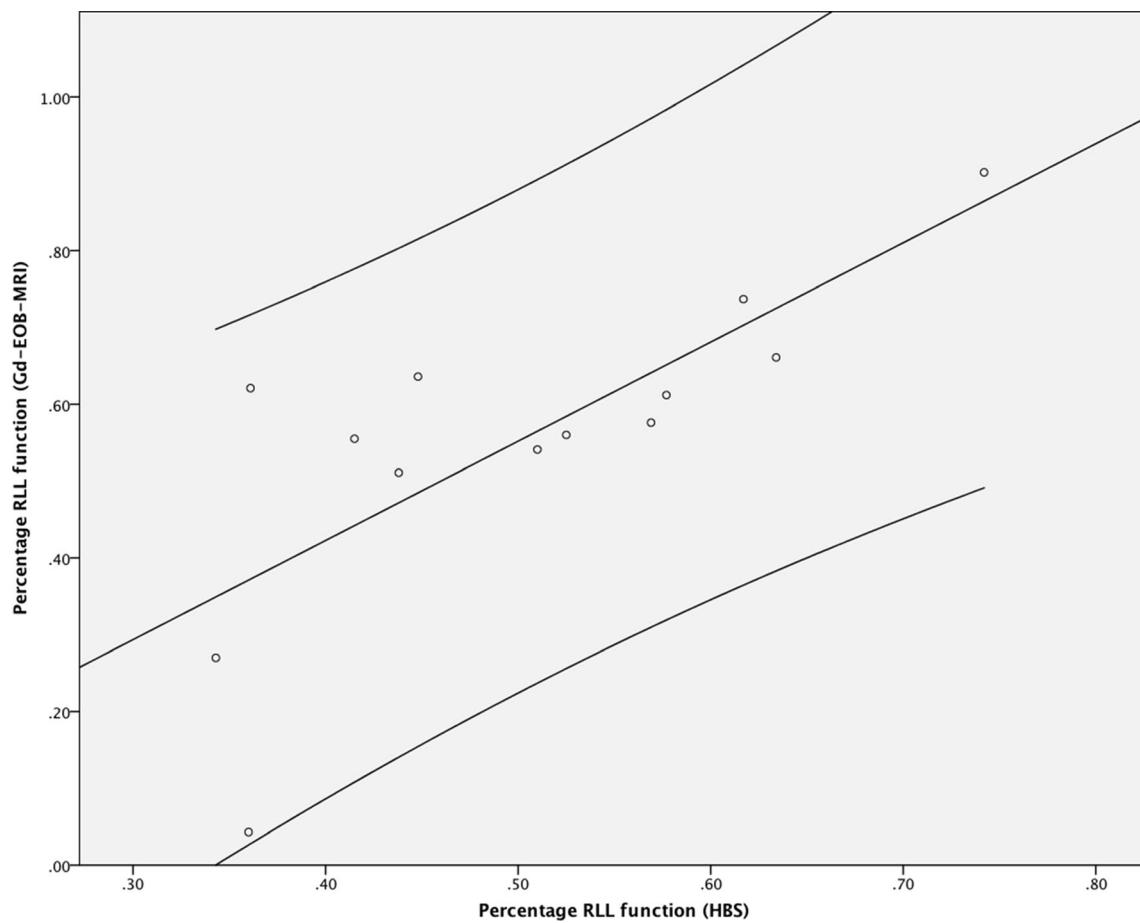
Fig. 3 Correlation of percentage RLL function as calculated from Gd-EOB-enhanced MRI using the proportion of HUI of RLL and LLL and percentage RLL function as calculated by mebrofenin uptake in ^{99m}Tc-mebrofenin hepatobiliary scintigraphy. Line of best fit and 95 % confidence intervals are shown as *straight* and *curved lines*, respectively

data acquisition in the anterior and posterior projection using a dual-head gamma camera and calculating geometric mean activity. The posterior view, however, is hampered by the unequal attenuation of tissues between the liver and the collimator, which is caused by the spine. Although this can be partially overcome by adding an additional fast SPECT acquisition during the dynamic phase [5], MRI should theoretically yield more accurate functional results because the three-dimensional data set is not subject to an attenuation bias and allows more exact separation of left and right liver lobe. This has to be verified in additional studies.

In conclusion our results suggest that Gd-EOB-enhanced MRI and ^{99m}Tc-mebrofenin HBS may equally be used to separately determine right and left liver lobe function after PVE.

References

1. Manizate F, Hiotis SP, Labow D, Roayaie S, Schwartz M (2010) Liver functional reserve estimation: state of the art and relevance for local treatments: the Western perspective. J Hepatobiliary Pancreatol Sci 4:385–388
2. de Graaf W, van Lienden KP, van Gulik TM, Bennink RJ (2010) (99m)Tc-mebrofenin hepatobiliary scintigraphy with SPECT for the assessment of hepatic function and liver functional volume before partial hepatectomy. J Nucl Med 2:229–236
3. Saito K, Ledsam J, Sourbron S et al (2012) Assessing liver function using dynamic Gd-EOB-DTPA-enhanced MRI with a standard 5-phase imaging protocol. J Magn Reson Imaging 37:1109–1114
4. Nilsson H, Nordell A, Vargas R, Douglas L, Jonas E, Blomqvist L (2009) Assessment of hepatic extraction fraction and input relative blood flow using dynamic hepatocyte-specific contrast-enhanced MRI. J Magn Reson Imaging 6:1323–1331

5. de Graaf W, van Lienden KP, van den Esschert JW, Bennink RJ, van Gulik TM (2011) Increase in future remnant liver function after preoperative portal vein embolization. Br J Surg 6:825–834

6. Erdogan D, Heijnen BH, Bennink RJ et al (2004) Preoperative assessment of liver function: a comparison of 99mTc-mebrofenin scintigraphy with indocyanine green clearance test. Liver Int 2:117–123

7. Yamada A, Hara T, Li F et al (2011) Quantitative evaluation of liver function with use of gadoxetate disodium-enhanced MR imaging. Radiology 3:727–733

8. Geisel D, Lüdemann L, Keuchel T et al (2013) Increase in left liver lobe function after preoperative right portal vein embolisation assessed with gadolinium-EOB-DTPA MRI. Eur Radiol 9:2555–2560

9. Neuhaus P, Thelen A, Jonas S et al (2012) Oncological superiority of hilar en bloc resection for the treatment of hilar cholangiocarcinoma. Ann Surg Oncol 5:1602–1608

10. Klatskin G (1965) Adenocarcinoma of the hepatic duct at its bifurcation within the porta hepatis: an unusual tumor with distinctive clinical and pathological features. Am J Med 2:241–256

11. Neuhaus P, Jonas S, Bechstein WO et al (1999) Extended resections for hilar cholangiocarcinoma. Ann Surg 6:808–818, discussion 819

12. Dinant S, Gerhards MF, Rauws EAJ, Busch ORC, Gouma DJ, van Gulik TM (2006) Improved outcome of resection of hilar cholangiocarcinoma (Klatskin tumor). Ann Surg Oncol 6:872–880

13. Agrawal S, Belghiti J (2011) Oncologic resection for malignant tumors of the liver. Ann Surg 4:656

14. Jonas S, Benckert C, Thelen A, Lopez-Hänninen E, Rösch T, Neuhaus P (2008) Radical surgery for hilar cholangiocarcinoma. Eur J Surg Oncol 3:263

15. Ekman M, Fjälling M, Holmberg S, Person H (1992) IODIDA clearance rate: a method for measuring hepatocyte uptake function. Transplant Proc 1:387–388

16. Ekman M, Fjälling M, Friman S, Carlson S, Volkmann R (1996) Liver uptake function measured by IODIDA clearance rate in liver transplant patients and healthy volunteers. Nucl Med Commun 3:235–242

17. de Graaf W, Bennink RJ, Veteläinen R, van Gulik TM (2010) Nuclear imaging techniques for the assessment of hepatic function in liver surgery and transplantation. J Nucl Med 5:742–752

18. Bennink RJ, Dinant S, Erdogan D et al (2004) Preoperative assessment of postoperative remnant liver function using hepatobiliary scintigraphy. J Nucl Med 6:965–971

19. de Graaf W, Bennink RJ, Heger M, Maas A, de Bruin K, van Gulik TM (2011) Quantitative assessment of hepatic function during liver regeneration in a standardized rat model. J Nucl Med 2:294–302

20. Nilsson H, Blomqvist L, Douglas L, Nordell A, Jonas E (2010) Assessment of liver function in primary biliary cirrhosis using Gd-EOB-DTPA-enhanced liver MRI. HPB (Oxford) 8:567–576

21. Shimizu J, Dono K, Gotoh M et al (1999) Evaluation of regional liver function by gadolinium-EOB-DTPA-enhanced MR imaging. Dig Dis Sci 7:1330–1337

22. Geisel D, Lüdemann L, Wagner C et al (2013) Evaluation of gadolinium-EOB-DTPA uptake after portal vein embolization: value of an increased flip angle. Acta Radiol 55(2):149–154

23. Gschwend S, Ebert W, Schultze-Mosgau M, Breuer J (2011) Pharmacokinetics and imaging properties of Gd-EOB-DTPA in patients with hepatic and renal impairment. Invest Radiol 9:556–566

24. Bennink RJ, Tulchinsky M, de Graaf W, Kadry Z, van Gulik TM (2012) Liver function testing with nuclear medicine techniques is coming of age. Semin Nucl Med 2:124–137

25. Kim HJ, Kim BS, Kim MJ et al (2012) Enhancement of the liver and pancreas in the hepatic arterial dominant phase: comparison of hepatocyte-specific MRI contrast agents, gadoxetic acid and gadobenate dimeglumine, on 3 and 1.5 tesla MRI in the same patient. J Magn Reson Imaging. doi:10.1002/jmri.23874

26. Wang H, Cao Y (2012) Correction of arterial input function in dynamic contrast-enhanced MRI of the liver. J Magn Reson Imaging 2:411–421

27. Kim T, Murakami T, Hasuike Y et al (1997) Experimental hepatic dysfunction: evaluation by MRI with Gd-EOB-DTPA. J Magn Reson Imaging 4:683–688

28. Nishie A, Asayama Y, Ishigami K et al (2012) MR prediction of liver fibrosis using a liver-specific contrast agent: superparamagnetic iron oxide versus Gd-EOB-DTPA. J Magn Reson Imaging 3:664–671

29. Morris-Stiff G, Gomez D, Prasad R (2009) Quantitative assessment of hepatic function and its relevance to the liver surgeon. J Gastrointest Surg 2:374–385

30. Tajima T, Takao H, Akai H et al (2010) Relationship between liver function and liver signal intensity in hepatobiliary phase of gadolinium ethoxybenzyl diethylenetriamine pentaacetic acid-enhanced magnetic resonance imaging. J Comput Assist Tomogr 3:362–366

31. Norén B, Forsgren MF, Dahlqvist Leinhard O et al (2012) Separation of advanced from mild hepatic fibrosis by quantification of the hepatobiliary uptake of Gd-EOB-DTPA. Eur Radiol 23:174–181

32. Dahlqvist Leinhard O, Dahlström N, Kihlberg J et al (2012) Quantifying differences in hepatic uptake of the liver specific contrast agents Gd-EOB-DTPA and Gd-BOPTA: a pilot study. Eur Radiol 3:642–653

33. Verloh N, Haimerl M, Zeman F et al (2014) Assessing liver function by liver enhancement during the hepatobiliary phase with Gd-EOB-DTPA-enhanced MRI at 3 Tesla. Eur Radiol 24:1013–1019

34. Yoneyama T, Fukukura Y, Kamimura K et al (2014) Efficacy of liver parenchymal enhancement and liver volume to standard liver volume ratio on Gd-EOB-DTPA-enhanced MRI for estimation of liver function. Eur Radiol 4:857–865

35. Kukuk GM, Schaefer SG, Fimmers R et al (2014) Hepatobiliary magnetic resonance imaging in patients with liver disease: correlation of liver enhancement with biochemical liver function tests. Eur Radiol 10:2482–2490

36. Geisel D, Lüdemann L, Gebauer B et al (2014) Optimized separation of left and right liver lobe in dynamic (99m)Tc-mebrofenin hepatobiliary scintigraphy using a hybrid SPECT-CT scanner. Ann Nucl Med 28:897–902

37. Ringe KI, Husarik DB, Sirlin CB, Merkle EM (2010) Gadoxetate disodium-enhanced MRI of the liver: part 1, protocol optimization and lesion appearance in the noncirrhotic liver. AJR Am J Roentgenol 1:13–28

38. Cruite I, Schroeder M, Merkle EM, Sirlin CB (2010) Gadoxetate disodium-enhanced MRI of the liver: part 2, protocol optimization and lesion appearance in the cirrhotic liver. AJR Am J Roentgenol 1:29–41

39. Michaely HJ, Morelli JN, Budjan J et al (2013) CAIPIRINHA-Dixon-TWIST (CDT)-volume-interpolated breath-hold examination (VIBE): a new technique for fast time-resolved dynamic 3-dimensional imaging of the abdomen with high spatial resolution. Invest Radiol 8:590–597